

Theoretical predictions on the clustering of SCUBA galaxies and implications for small-scale fluctuations at sub-mm wavelengths

M. Magliocchetti¹, L. Moscardini², P. Panuzzo¹, G. L. Granato³, G. De Zotti³, L. Danese¹

¹ *SISSA, Via Beirut 4, 34100, Trieste, Italy*

² *Dipartimento di Astronomia, Università di Padova, Vicolo dell'Osservatorio 5, I-35122 Padova, Italy*

³ *Osservatorio Astronomico, Vicolo dell'Osservatorio 5, I-35122 Padova, Italy*

16 November 2018

ABSTRACT

This paper investigates the clustering properties of SCUBA-selected galaxies in the framework of a unifying scheme relating the formation of QSOs and spheroids (Granato et al. 2000). The theoretical angular correlation function is derived for different bias functions, corresponding to different values of the ratio $M_{\text{halo}}/M_{\text{sph}}$ between the mass of the dark halo and the final mass in stars. SCUBA sources are predicted to be strongly clustered, with a clustering strength increasing with mass. We show that the model accounts for the clustering of Lyman-break Galaxies, seen as the optical counterpart of low- to intermediate-mass primeval spheroidal galaxies and is also consistent with the observed angular correlation function of Extremely Red Objects. Best agreement is obtained for $M_{\text{halo}}/M_{\text{sph}} = 100$. We also consider the implications for small scale fluctuations observed at sub-mm wavelengths by current or forthcoming experiments aimed at mapping the Cosmic Microwave Background (CMB). The predicted amplitude of the clustering signal in the 350 GHz channel of the Planck mission strongly depends on the halo-to-bulge mass ratio and may be of comparable amplitude to primary CMB anisotropies for multipole numbers $l \gtrsim 50$.

Key words: galaxies: clustering - galaxies: infrared - cosmology: theory - large-scale structure - cosmology: cosmic microwave background

1 INTRODUCTION

The advent of the 450-850 μm Submillimetre Common User Bolometric Array (SCUBA) camera (Holland et al. 1999) has opened the possibility of exploiting the enormous potential of sub-mm astronomy for investigating the early phases of galaxy evolution, taking advantage of the strongly negative K-correction which boosts the visibility of high- z galaxies (Smail, Ivison & Blain 1997; Barger et al. 1998; Hughes et al. 1998; Barger, Cowie & Sanders 1999; Eales et al. 1999; Blain et al. 1999a).

A variety of models has been proposed to reproduce the properties of the submillimetre population (e.g. Guiderdoni et al. 1998; Blain et al. 1999b; Devriendt, Guiderdoni & Sadat 1999; Devriendt & Guiderdoni 2000; Takeuchi et al. 2000; Pearson 2000), in particular the dramatic star-formation rate inferred from the data.

Granato et al. (2000 - hereafter Paper I) propose a unified scheme for the formation of the QSO and spheroidal population. According to their model, at the time of the onset of the QSO activity, the host galaxy has already under-

gone a major star-formation event, with a characteristic time T_B ranging from ~ 0.5 to ~ 2 Gyr when going from more to less massive hosts. The QSO onset practically stops the star-formation process, and when eventually the reservoir of gas fueling the Active Galactic Nuclei is exhausted, the host galaxy will evolve in a passive way, with a spectrum becoming quickly red. This approach identifies SCUBA galaxies as the progenitors of QSO hosts and provides an excellent description of (amongst others) the observed 850 μm number counts.

In this paper we present predictions on clustering properties of SCUBA galaxies in the framework of the Granato et al. (2000) model. Such properties are determined by the combination of the evolution of the underlying mass fluctuations and the bias relating galaxy overdensities to mass. Since the bias factor is determined by properties related to the process of galaxy formation, it follows that measurements of clustering can lead to very precious insights on the galaxy population producing the signal.

Unfortunately the number of SCUBA galaxies observed

is still too small to allow for any clustering measurement. The model by Granato et al. (2000) however establishes a tight link between this population and Lyman-break galaxies (Steidel et al. 1996; LBGs hereafter), interpreted as lower-mass/lower-submm luminosity sources. Such model can thus be tested against measurements of LBG clustering (Giavalisco et al. 1998). A further test is provided by the recent detection (Daddi et al. 2000) of strong clustering of Extremely Red Objects (EROs), which were found to be the optical counterparts of two of the still few SCUBA sources having reliable optical identifications (Smail et al. 1999).

An important issue related to the above discussion is the effect of clustering on small scale anisotropies at mm/sub-mm wavelengths, where experiments to map the Cosmic Microwave Background either have been (e.g. BOOMERanG, MAXIMA, TopHat, ACBAR, ARCHEOPS) or are about to be carried out (notably the ESA's Planck mission). Small scale fluctuations of the background intensity due to clustering of unresolved sources are proportional to the amplitude of their two-point correlation function and to their volume emissivity (see, e.g., De Zotti et al. 1996). The deep SCUBA surveys have demonstrated that the bulk of the extragalactic background at 850 μm comes from a relatively small number of sources (at least ten times less than those accounting for the bulk of the optical/UV background) at substantial redshifts. Combining the (rather limited) direct spectroscopic information (e.g. Frayer 2000) with estimates based on the sub-mm to radio spectral index (Carilli & Yun 1999), it is concluded that the median redshift of the sub-mm population brighter than $\sim 1\text{ mJy}$ is probably $\sim 2.5\text{--}3$ (Smail et al. 2000). It then follows that most of the background comes from a population of extremely luminous (hence presumably very massive) high- z galaxies which probably correspond to the rare, high density peaks in the primordial matter distribution. The standard structure formation scenario predicts that these peaks are strongly clustered (Kaiser 1984; Baron & White 1987). Also, according to the currently favoured view, SCUBA sources probably correspond to the phase of intense star formation in large spheroidal galaxies, a process that appears to be completed for $z > 1$; as a consequence, the relevant redshift range is limited and dilution of the clustering signal is relatively small.

The amplitude of intensity fluctuations due to clustering is correspondingly expected to be large. Scott & White (1999) worked out a preliminary estimate adopting for sub-mm sources the angular correlation function determined for $z \sim 3$ LBGs (which however are mostly undetectable by SCUBA; see Chapman et al. 2000). Here we provide quantitative estimates of this effect using a technique developed by Peacock & Dodds (1996), Matarrese et al. (1997) and Moscardini et al. (1998), which takes into account the effects of the past light-cone, the linear and non-linear growth of clustering and the evolution of the bias factor. The epoch-dependent mass distribution of sources is modelled following Granato et al. (2000).

The plan of the paper is as follows. Section 2 will be devoted to the analysis of the clustering of SCUBA galaxies and comparisons with the observed clustering properties of LBGs and EROs, while in Section 3 we use the findings of Section 2 to make predictions on the temperature fluctuations produced by unresolved SCUBA-like sources and to

discuss their implications for experiments aimed at mapping the CMB at sub-mm wavelengths. Section 4 summarizes our conclusions.

Throughout the paper we will assume a cosmological model with $h_0 = 0.7$, $\Omega_0 = 0.3$, $\Lambda = 0.7$, and adopt the normalization of the rms mass fluctuation $\sigma_8 = 1$ determined by the 4-year COBE data (Bunn & White 1997).

2 CLUSTERING OF SCUBA SOURCES

The angular two-point correlation function $w(\theta)$ is defined as the excess probability, δP , with respect to a random Poisson distribution, of finding two sources in the solid angles $\delta\Omega_1$ $\delta\Omega_2$ separated by an angle θ , and it is defined by

$$\delta P = n^2 \delta\Omega_1 \delta\Omega_2 [1 + w(\theta)] \quad (1)$$

where n is the mean number density of objects in the particular catalogue under consideration.

The theoretical expression for $w(\theta)$ can be derived from its spatial counterpart ξ by projection via the relativistic Limber equation (Peebles 1980):

$$w(\theta) = 2 \frac{\int_0^\infty \int_0^\infty N^2(z) b_{\text{eff}}^2(M_{\text{min}}, z) (dz/dx) \xi(r, z) dz du}{\left[\int_0^\infty N(z) dz \right]^2}, \quad (2)$$

where x is the comoving radial coordinate, $r = (u^2 + x^2 \theta^2)^{1/2}$ (for a flat universe and in the small angle approximation: $\theta \ll 1$ rad), and $N(z)$ is the number of objects within the shell $(z, z + dz)$.

The mass-mass correlation function $\xi(r, z)$ to be inserted in eq.(2) has been obtained following the work by Peacock & Dodds (1996, but also see Magliocchetti et al., 2000), extended by Matarrese et al. (1997) and Moscardini et al. (1998) to redshifts $z > 0$, which provides an analytical way to derive the trend of $\xi(r, z)$ both in the linear and non-linear regime. Note that $\xi(r, z)$ only depends on the underlying cosmology and on the normalization of σ_8 . The relevant properties of SCUBA galaxies are included in the redshift distribution of sources $N(z)$, where $N(z) dz$ gives the number of objects in the shell $(z, z + dz)$ (given in Paper I and shown in Fig. 1 for fluxes respectively greater than 1, 10, 50 mJy), and in the bias factor $b_{\text{eff}}(M_{\text{min}}, z)$.

The effective bias factor $b_{\text{eff}}(M_{\text{min}}, z)$ of all haloes with masses greater than some threshold M_{min} is obtained by integrating the quantity $b(M, z)$ - representing the bias of individual haloes of mass M - opportunely weighted by the number density $n_{\text{SCUBA}}(M, z)$ of SCUBA sources:

$$b_{\text{eff}}(z) = \frac{\int_{M_{\text{min}}}^\infty dM b(M, z) n_{\text{SCUBA}}(M, z)}{\int_{M_{\text{min}}}^\infty dM n_{\text{SCUBA}}(M, z)}. \quad (3)$$

Note that as n_{SCUBA} can be thought as the fraction of haloes hosting a galaxy in the process of forming stars, its expression can also be written as $n_{\text{SCUBA}}(M, z) = n(M, z) T_B/t_h$, where $n(M, z) dM$ is the mass spectrum of haloes with masses between M and $M + dM$ (Press & Schechter, 1974; Sheth & Tormen, 1999), T_B is the duration of the star-formation burst and t_h is the life-time of the haloes in which these objects reside (see Martini & Weinberg, 2000). The duration of the star-formation phase T_B varies with the mass of the spheroid undergoing the burst (see Paper I), assuming a value $T_b = 0.5$ Gyr in the case of massive objects (i.e. with

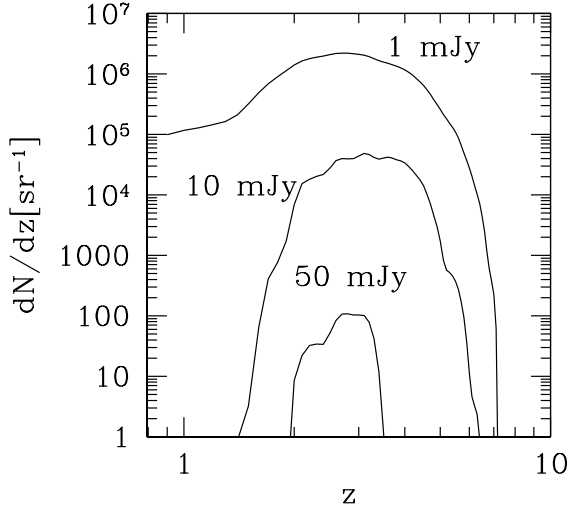


Figure 1. Predicted redshift distribution for SCUBA galaxies respectively brighter than 1, 10 and 50 mJy. The Figure is adapted from Paper I.

bulge masses $M_{\text{sph}} \gtrsim 1.5 \cdot 10^{11} M_{\odot}$) and increasing when going to lower masses.

We take the expression for $b(M, z)$ to be plugged into eq.(3) from Jing (1998):

$$b(M, z) = \left(1 + \frac{1}{\delta_c} \left[\frac{\delta_c^2(z)}{\sigma^2(M)} - 1 \right] \right) \left(\frac{\sigma^4(M)}{2 \delta_c^4(z)} + 1 \right)^{\frac{(6-2n_{\text{eff}})}{100}} \quad (4)$$

with $\delta_c(z) = \delta_c/D(z)$, $D(z)$ being the linear growing factor and δ_c the critical density for collapse of a homogeneous spherical perturbation ($\delta_c = 1.686$ in an Einstein-de Sitter universe). $\sigma^2(M)$ is the variance of density fluctuations on the mass scale M , and $n_{\text{eff}} = -3 - 6(d \ln \sigma / d \ln M)$. Note that the assumption of a linear bias is justified by the redshift distribution of the sources, all appearing for $z \gtrsim 0.75$ (see e.g. Somerville et al., 2001).

According to Granato et al. (2000), sources showing up in the SCUBA counts can be broadly divided into three categories: low-mass (masses in the range $M_{\text{sph}} \simeq 10^9 - 10^{10} M_{\odot}$, duration of the star formation burst $T_B \sim 2$ Gyr, and typical fluxes $S \lesssim 1$ mJy), intermediate-mass ($M_{\text{sph}} \simeq 10^{10} - 10^{11} M_{\odot}$ and $T_B \sim 1$ Gyr) and high-mass ($M_{\text{sph}} \gtrsim 10^{11} M_{\odot}$, $T_B \sim 0.5$ Gyr, dominating the counts at fluxes $S \gtrsim 5 - 10$ mJy). Note that by M_{sph} we denote the mass in stars at completion of the star formation process.

In order to evaluate the bias factor in eq.(3) we then consider two extreme cases for the ratio between the mass in stars and the mass of the host dark halo: $M_{\text{halo}}/M_{\text{sph}} = 100$ and $M_{\text{halo}}/M_{\text{sph}} = 10$. Note that $M_{\text{halo}}/M_{\text{sph}} = 10$ roughly corresponds to the ratio $\Omega_0/\Omega_{\text{baryon}}$ between total and baryon density, where we adopted for the latter quantity the standard value from primordial nucleosynthesis; this corresponds to having assumed all the baryons to be locked into stars and, as a consequence, gives a conservative lower limit to the quantity $M_{\text{halo}}/M_{\text{sph}}$. $M_{\text{halo}}/M_{\text{sph}} = 100$ is instead related to Ω_0/Ω_* , Ω_* being the present mass density in visible

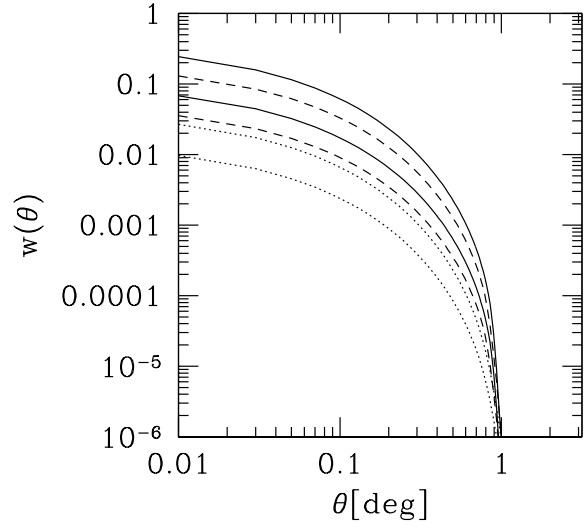


Figure 2. Predictions for the angular correlation function $w(\theta)$ for different halo-to-bulge mass ratios and different flux cuts. Solid lines are for sources brighter than 50 mJy, dashed lines for sources brighter than 10 mJy, while dotted lines correspond to $S \geq 1$ mJy. Higher curves of each type correspond to $M_{\text{halo}}/M_{\text{sph}} = 100$, lower ones to $M_{\text{halo}}/M_{\text{sph}} = 10$.

stars (Persic & Salucci, 1992; Fukugita et al. 1998). The likely value should be $M_{\text{sph}}/M_{\text{halo}} = 1 - 3 \%$ (cf. Paper I).

Armed with the above results we can finally evaluate the two-point correlation function in eq. (2) for different $M_{\text{halo}}/M_{\text{sph}}$ ratios and different flux cuts. Figure 2 presents our predictions for $w(\theta)$, respectively for a flux cut of 50 (solid line), 10 (dashed line) and 1 (dotted line) mJy. Higher curves of each kind correspond to the case $M_{\text{halo}}/M_{\text{sph}} = 100$, while lower curves refer to the $M_{\text{halo}}/M_{\text{sph}} = 10$ one.

The highest clustering amplitude is found for the brightest sources ($S \geq 50$ mJy). This is because they are associated to the most massive dark halos and are therefore highly biased tracers of the dark matter distribution. In addition, according to the model by Granato et al. (2000), they have a rather narrow redshift distribution (see Fig. 1), so that the dilution of the clustering signal is minimum.

The very sharp drop of all the curves at $\theta \simeq 1^\circ$ is due to the absence of nearby ($z \lesssim 1$, see Fig. 1) objects. This reflects the notion that the actively star-forming phase in spheroids is completed at $z > 1$.

The model introduced in Paper I establishes a strong link between SCUBA sources and LBGs where this latter population is predicted to be the low- to intermediate-mass tail of primeval spheroidal galaxies, with $T_B \sim 1 - 2$ Gyr and a star-formation rate ranging from a few to a hundred $M_{\odot} \text{ yr}^{-1}$.

Measurements of the angular correlation function of LBGs (Giavalisco et al. 1998) then offer a way to test such model. In Fig. 3 we plotted the expected $w(\theta)$ for sources with $S \geq 1$ mJy (corresponding to $M_{\text{sph}} \gtrsim 10^{10} M_{\odot}$) within the redshift range $2.5 \leq z \leq 3.5$, covered by the Giavalisco et al. (1998) sample. As in Fig. 2, the higher curve is for $M_{\text{halo}}/M_{\text{sph}} = 100$, the lower one for $M_{\text{halo}}/M_{\text{sph}} = 10$. The

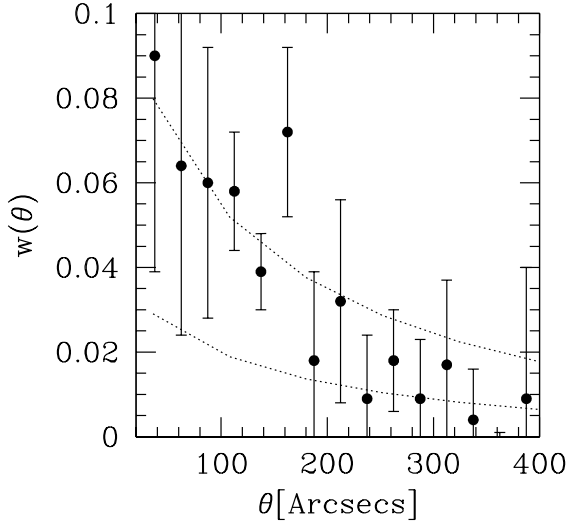


Figure 3. Angular correlation function of LBGs. Model predictions are shown by the dotted lines (the higher one is for $M_{\text{halo}}/M_{\text{sph}} = 100$, the lower for $M_{\text{halo}}/M_{\text{sph}} = 10$), while data points represent the Giavalisco et al. (1998) measurements.

data points show the Giavalisco et al. (1998) measurements. Despite the large errors, it is clear that the predicted trend for $w(\theta)$ correctly reproduces the data, a better fit obtained for $M_{\text{halo}}/M_{\text{sph}} = 100$. This result, apart from providing a further proof of the tight link between SCUBA galaxies and LBGs, also confirms the expectations of Paper I for a small fraction (on the order of a few percent) of the total mass to be confined into stars.

Strong clustering of EROs has been recently detected by Daddi et al. (2000). This result may again provide a relevant test for our model since it seems likely for a substantial fraction of SCUBA galaxies to be EROs with $R-K \geq 6$: at least two out of nine ($> 20\%$) sources in the Cluster Lens Survey belong to this class (Smail et al. 1999), while other submillimeter surveys have discovered additional EROs as counterparts of SCUBA sources (Iverson et al. 2000). For their ERO sample with $K_s < 19.2$ and $R - K_s \geq 5.3$, Daddi et al. (2000) find $w(\theta) \simeq 0.07$ for $\theta \simeq 0^\circ.1$, not far from the predictions in Fig. 2.

3 SMALL SCALE FLUCTUATIONS FROM DISCRETE SOURCES

3.1 The Intensity Correlation Function

An issue intimately connected with the analysis of galaxy clustering performed in the previous Section is the study of the contribution of unresolved sources (i.e. sources with fluxes fainter than some detection limit S_d) to the background intensity. Its general expression is:

$$I = \int_0^{S_d} \frac{dN}{dS} S dS = \frac{1}{4\pi} \int_{L_{\min}}^{L_{\max}} d\log L L \int_{z(S_d, L)}^{z_{\max}} dz \Phi(L, z) \frac{K(L, z)}{(1+z)^2} \frac{dx}{dz} \quad (5)$$

(see e.g. De Zotti et al. 1996), where dN/dS denotes the differential number counts, L_{\max} and L_{\min} are respectively the maximum and minimum local luminosity of the sources, $K(L, z) = (1+z)L[\nu(1+z)]/L(\nu)$ is the K-correction, z_{\max} is the redshift when the sources begin to shine, $z(S_d, L)$ is the redshift at which a source of luminosity L is seen with a flux equal to the detection limit S_d , $\Phi(L, z)$ is the luminosity function (i.e. the comoving number density of sources per unit $d\log L$), and x is the comoving radial coordinate.

The intensity fluctuation δI due to inhomogeneities in the space distribution of unresolved sources is then given by eq. (5), with the quantity $\Phi(L, z)$ replaced by $\delta\Phi(L, z)$. It is easily shown that the angular correlation of such intensity fluctuations

$$C(\theta) = \langle \delta I(\theta', \phi') \delta I(\theta'', \phi'') \rangle, \quad (6)$$

where (θ', ϕ') and (θ'', ϕ'') define two positions on the sky separated by an angle θ , can be expressed as the sum of two terms C_P and C_C , the first one due to Poisson noise (i.e. fluctuations given by randomly distributed objects), and the second one owing to source clustering.

Scott & White (1999) have shown that if dusty galaxies cluster like LBGs (Giavalisco et al. 1998), anisotropies due to clustering dominate the Poisson ones at all angular scales. According to our model, LBGs are the optical counterparts of the low- to intermediate- mass tail of SCUBA galaxies; as illustrated in Figure 2, this makes the clustering signal of LBGs a factor ~ 10 lower than the one obtained for SCUBA galaxies; therefore we can safely assume the Poisson term C_P to be negligible in the following analysis and only concentrate on temperature fluctuations caused by the C_C term (hereafter simply called C).

By making use of the quantities defined in Section 2 and of eq. (5), the clustering term in eq. (6) takes the form:

$$C(\theta) = \left(\frac{1}{4\pi}\right)^2 \int_{z(L_{\min}, S_d)}^{z_{\max}} dz b_{\text{eff}}^2(z) \frac{j_{\text{eff}}^2(z)}{(1+z)^4} \left(\frac{dx}{dz}\right)^2 \int_0^\infty du \xi(r, z), \quad (7)$$

where

$$j_{\text{eff}} = \int_{L_{\min}}^{\min[L_{\max}, L(S_d, z)]} \Phi(L, z) K(L, z) L d\log L \quad (8)$$

is the effective volume emissivity (see Toffolatti et al. 1998).

Following the prescriptions of Section 2, we have then evaluated $C(\theta)$ in eq.(7) separately for the three cases of low-, intermediate- and high-mass objects, by plugging in eq. (8) the appropriate expressions for the luminosity function. Note that in this case, the quantity $b^2(M_{\min}, z)$ should indeed be read as $b^2(M_{\min}, M_{\max}, z)$, where M_{\max} is the maximum halo mass corresponding to the maximum visible bulge mass (i.e. upper limit for the mass locked into stars whose values are given in Section 2). This corresponds in eq.(3) to a replacement in the upper limit of the integrals of ∞ with M_{\max} .

Figure 4 shows predictions for the correlation signal due to intensity fluctuations (in units $\text{ergs}^2 \text{cm}^{-4} \text{Hz}^{-2} \text{sr}^{-2}$) in the case of SCUBA galaxies. Dotted, dashed and solid lines are respectively for spheroids of $M_{\text{sph}}^{\text{min}} = 10^9$, 10^{10} and $10^{11} M_\odot$. In each plot the two solid curves correspond to different detection limits, the 100 mJy case represented by the higher curve and the 10 mJy case by the lower one. Note that, due to the steepness of the bright end of source

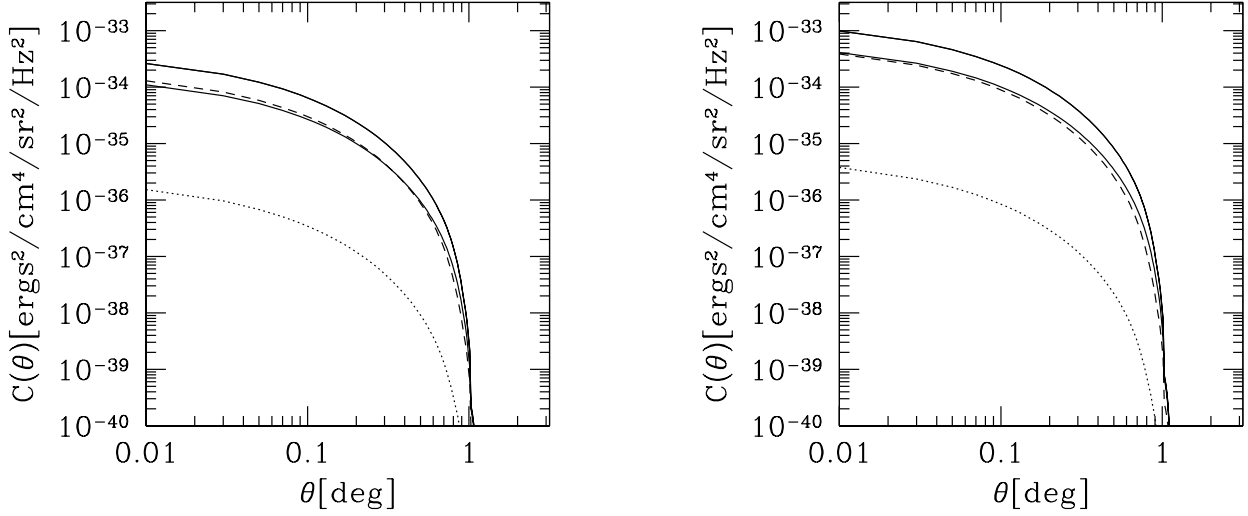


Figure 4. Left panel: predictions for the correlation signal due to intensity fluctuations of SCUBA galaxies in the case $M_{\text{halo}}/M_{\text{sph}} = 10$. Dotted, dashed and solid lines are respectively for spheroids of low ($M_{\text{sph}} = 10^9\text{--}10^{10} M_{\odot}$), intermediate ($M_{\text{sph}} = 10^{10}\text{--}10^{11} M_{\odot}$), and high ($M_{\text{sph}} > 10^{11} M_{\odot}$) masses. The two solid curves are obtained for different flux detection limits, the 100 mJy case represented by the higher curve and the 10 mJy case by the lower one. Right panel: same as before but with a ratio $M_{\text{halo}}/M_{\text{sph}} = 100$.

counts, the results are independent of S_d if $S_d \geq 100$ mJy. Results are shown for $M_{\text{halo}}/M_{\text{sph}} = 10$ (left-hand panel) and $M_{\text{halo}}/M_{\text{sph}} = 100$ (right-hand panel). Note once again the steep drop of all the curves around $\theta \simeq 1^\circ$ caused by the absence of nearby sources of this kind and the very small contribution given by the low-mass objects, mostly due to their small bias function and their modest contribution to the effective volume emissivity.

In order to evaluate the total contribution of the clustering to intensity fluctuations one has to add up all the values of $C(\theta)$ in eq. (7) obtained for the different mass intervals and also to take into account the cross-correlation terms between objects of different masses, so that the final expression for $C(\theta)$ is given by

$$C^{\text{TOT}}(\theta) = \sum_{i,j=1}^3 \sqrt{C_i(\theta)C_j(\theta)}, \quad (9)$$

where the indexes i, j stand for high, intermediate and low masses.

3.2 Power Spectrum of Temperature Fluctuations

The angular power spectrum of the intensity fluctuations [eqs. (7)–(9)] can be obtained starting from the well known expression for the expansion of temperature fluctuations in spherical harmonics

$$\frac{\delta T}{T}(\theta, \phi) = \sum_{l=0}^{\infty} \sum_{m=-l}^l a_l^m Y_l^m(\theta, \phi). \quad (10)$$

If the fluctuations are a stationary process it can be shown (Peebles 1993) that the previous expression does not depend

on the index m (i.e. on the ϕ angle), so that we can write:

$$C_l = \frac{1}{2l+1} \sum_{m=-l}^l \langle |a_l^m|^2 \rangle = \langle |a_l^0|^2 \rangle, \quad (11)$$

with

$$a_l^0 = \int_0^{2\pi} \int_0^\pi \frac{\delta T(\theta)}{T} \sqrt{\frac{2l+1}{4\pi}} P_l(\cos\theta) \sin\theta \, d\theta \, d\phi \quad (12)$$

(see Toffolatti et al. 1998), where $P_l(\cos\theta)$ are the Legendre polynomials, and $\delta T/T$ is expressed as

$$\frac{\delta T}{T}(\theta) = \left\langle \left(\frac{\Delta T}{T} \right)^2 \right\rangle^{1/2} = \frac{\lambda^2 \sqrt{C^{\text{TOT}}(\theta)}}{2 k_b T} \left[\exp\left(\frac{h\nu}{k_b T}\right) - 1 \right]^2 \times \exp\left(-\frac{h\nu}{k_b T}\right) / \left(\frac{h\nu}{k_b T}\right)^2, \quad (13)$$

which relates intensity and temperature fluctuations ($T=2.726$ K, Mather et al. 1994).

Figure 5 shows the predicted values for the quantity $\delta T_l = \sqrt{l(l+1)C_l}/2\pi$ (in units of K) at 353 GHz (850 μm) - the central frequency of one of the channels of the High Frequency Instrument (HFI) of the ESA's Planck mission - as a function of the multipole l up to $l = 1000$. Results are plotted for two values of the source detection limit ($S_d = 100$ and 10 mJy; note that the source detection limit for this Planck channel is likely to be > 100 mJy) and the usual two values of $M_{\text{halo}}/M_{\text{sph}}$. Also shown, for comparison, is the power spectrum of primary (CMB) anisotropies (solid line) predicted by a standard Cold Dark Matter model for a Λ CDM ($\Lambda = 0.7$, $\Omega_0 = 0.3$, $h_0 = 0.7$), computed with the CMBFAST code developed by Seljak & Zaldarriaga (1996).

At this frequency our model predicts fluctuations of amplitude due to clustering comparable to (and possibly even larger than) those obtained for primary CMB anisotropies at $l \gtrsim 50$. As illustrated by Fig. 4, most of the clustering

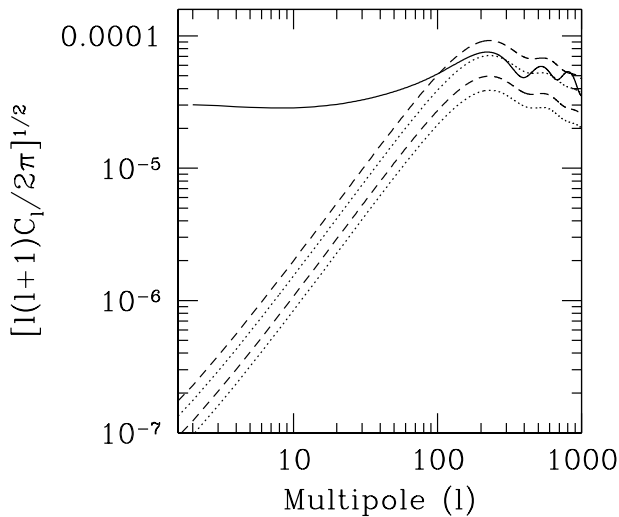


Figure 5. Predicted power spectrum of temperature fluctuations $\delta T_l = \sqrt{l(l+1)C_l/2\pi}$ (in units of K) as a function of the multipole l at 353 GHz, the central frequency of a Planck/HFI channel. The dashed lines are for a detection limit $S_d = 100$ mJy, the dotted ones for $S_d = 10$ mJy. In both cases the higher curves are obtained for $M_{\text{halo}}/M_{\text{sph}}=100$, the lower ones for $M_{\text{halo}}/M_{\text{sph}}=10$. The solid line represents the power spectrum of primary CMB anisotropies as predicted by a standard Cold Dark Matter model for a Λ CDM cosmology ($\Lambda = 0.7$, $\Omega_0 = 0.3$, $h_0 = 0.7$).

signal comes from massive galaxies with fluxes $S \gtrsim 1$ mJy, which lie at substantial redshifts (see Fig. 1) and are therefore highly biased tracers of the underlying mass distribution. Also the strongly negative K-correction increases their contribution to the effective volume emissivity [eq. (8)] and therefore to the fluctuations.

We therefore expect this effect to give a substantial contribution to the power spectrum extracted e.g. from the BOOMERanG map (de Bernardis et al. 2000) at 400 GHz. For $l \gtrsim 200$ its contribution may be comparable to that due to inhomogeneous emission by the interstellar dust.

4 CONCLUSIONS

We have worked out predictions for the clustering properties of SCUBA-selected galaxies in the framework of an astrophysically grounded model, relating the formation of QSOs and spheroids (ellipticals, S0 galaxies and bulges of spirals). The theoretical angular correlation function has been derived for different bias functions, corresponding to different values of the ratio $M_{\text{halo}}/M_{\text{sph}}$ between the mass of a spheroid locked in stars and the mass of its host halo.

SCUBA sources are predicted to be strongly clustered, with a clustering strength which increases with increasing mass (or equivalently with increasing luminosity), as a consequence of the fact that they are very massive and shining at substantial redshifts. Since the clustering amplitude strongly depends on the quantity $M_{\text{halo}}/M_{\text{sph}}$, future measurements of the angular correlation function $w(\theta)$ will be able to discriminate amongst different models of SCUBA

galaxies and in particular to determine the amount of baryonic mass actively partaking the process of star formation.

Under the hypothesis of low- to intermediate-mass primeval spheroids to show up in the optical band as LBGs (as argued by Granato et al. 2000), we have then compared our predictions with the clustering measurements obtained by Giavalisco et al. (1998) for a wide sample of LBGs at $z \simeq 3$. The agreement is good for a mass ratio between the dark halo and the stellar component in the range 10–100; high values for this ratio seem to be favoured.

Also, the predicted amplitude of the angular correlation function of SCUBA galaxies is consistent with the one determined by Daddi et al. (2000) for EROs with $R-K_s \geq 5.3$ and $K_s \leq 19.2$. This would support the observational evidence for a substantial fraction of SCUBA galaxies to be identified with EROs (Smail et al. 1999; Ivison et al. 2000).

We have also considered the effect of clustering on maps of the Cosmic Microwave Background at sub-mm wavelengths, with special attention to the 353 GHz (850 μm) channel of the High Frequency Instrument (HFI) of the ESA’s Planck mission. The possibility of large fluctuations due to clustering at this (and also shorter) wavelength was first pointed out by Scott & White (1999) who adopted a phenomenological approach, assuming for SCUBA galaxies the clustering amplitudes observed for LBGs (Giavalisco et al. 1996). Our treatment, leading to a derivation of the angular autocorrelation function in the framework of the currently standard hierarchical clustering scenario, indicates that massive SCUBA galaxies (expected to dominate the population of sources sampled at fluxes $S \gtrsim 10$ mJy) are likely to be even more strongly clustered than LBGs. The corresponding fluctuations are then expected to be, at $\simeq 350$ GHz, of an amplitude comparable with those due to primary CMB anisotropies for multipole numbers $l > 50$. This would imply that important information on the clustering properties of faint sub-mm galaxies (and hence on their physical properties such as their mass and/or the amount of baryons involved in the star-formation process) resides in the BOOMERanG maps at 400 GHz where, however, the dominant signal is expected to come from interstellar dust emission. On the other hand, if the ratio $M_{\text{halo}}/M_{\text{sph}}$ is large, we expect the clustering signal to be comparable with dust emission fluctuations at $l \gtrsim 200$. It might therefore be possible to separate these two contributions and possibly exploit the different shapes of their power spectra.

As stressed by Scott & White (1999), the amplitude of the clustering signal drops rapidly - in comparison to the one arising from primary anisotropies - with decreasing frequency. In the nearest Planck/HFI channel (centered at 217 GHz) its contamination on the CMB anisotropy maps should already be negligible.

ACKNOWLEDGMENTS

Mauro Giavalisco is warmly thanked for providing us with the data shown in Figure 3. We are grateful to Pierluigi Monaco for useful clarifications on the relationship between SCUBA galaxies and quasars. We also thank ASI and Italian MURST for financial support.

REFERENCES

- Barger A.J., Cowie L.L., Sanders D.B., Fulton E., Taniguchi Y., Sato Y., Kawara K., Okuda H., 1998, *Nature*, 394, 248
- Barger A.J., Cowie L.L., Sanders D.B., 1999, *ApJ*, 518, L5
- Baron E., White S.D.M., 1987, *ApJ*, 322, 585
- Blain A.W., Kneib J.-P., Ivison R.J., Smail I., 1999a, *ApJ*, 512, L87
- Blain A.W., Jameson A., Smail I., Longair M.S., Kneib J.-P., Ivison R.J., 1999b, *MNRAS*, 309, 715
- Bunn E.F., White M., 1997, *ApJ*, 480, 6
- Carilli C.L., Yun M.S., 1999, *ApJ*, 513, L13
- Chapman S.C., Scott D., Steidel C.C., Borys C., Halpern M., Morris S.L., Aldeberger K.L., Dickinson M., Giavalisco M., Pettini M., 2000, *MNRAS*, 319, 318
- Daddi E., Cimatti A., Pozzetti L., Hoekstra H., Röttgering H.J.A., Renzini A., Zamorani G., Mannucci F., 2000, *A&A*, in press, astro-ph/0005581
- de Bernardis P., et al., 2000, *Nat*, 404, 995
- Devriendt J.E.G., Guiderdoni B., 2000, *A&A*, 363, 851
- Devriendt J., Guiderdoni B., Sadat R., 1999, *A&A*, 350, 381
- De Zotti G., Franceschini A., Toffolatti L., Mazzei P., Danese L., 1996, *Ap. Lett. Comm.*, 35, 289
- Eales S.A., Lilly S.J., Gear W.K., Dunne L., Bond J.R., Hammer F., Le Fevre O., Crampton D., 1999, *ApJ*, 515, 518
- Frazer D.T., 2000, in proc. UMass/INAOE Conf. on. "Deep Millimeter Surveys: Implications for Galaxy Formation and Evolution", World Scientific, in press, astro-ph/0007334
- Fukugita M., Hogan C.J., Peebles P.J.E., 1998, *ApJ*, 503, 518
- Giavalisco M., Steidel C.C., Adelberger K.L., Dickinson M.E., Pettini M., Kellogg M., 1998, *ApJ*, 503, 543
- Granato G.L., Silva L., Monaco P., Panuzzo P., Salucci P., De Zotti G., Danese L., 2000, *MNRAS*, submitted, astro-ph/9911304 - Paper I
- Guiderdoni B., Hivon E., Bouchet F.R., Maffei B., 1998, *MNRAS*, 295, 877
- Holland W.S. et al., 1999, *MNRAS*, 303, 659
- Hughes D.H. et al., 1998, *Nature*, 394, 241
- Ivison R.J., Dunlop J.S., Smail I., Dey A., Lui M.C., Graham J.A., 2000, *ApJ*, in press
- Jing Y.P., 1998, *ApJ*, 503, L9
- Kaiser N., 1984, *ApJ*, 284, L9
- Magliocchetti M., Bagla J., Maddox S.J., Lahav O., 2000, *MNRAS*, 314, 546
- Martini P., Weinberg D.H., 2000, astro-ph/0002384
- Matarrese S., Coles P., Lucchin F., Moscardini L., 1997, *MNRAS*, 286, 115
- Mather J.C. et al., 1994, *ApJ*, 420, 439
- Moscardini L., Coles P., Lucchin F., Matarrese S., 1998, *MNRAS*, 299, 95
- Peacock J.A., Dodds S.J., 1996, *MNRAS*, 267, 1020
- Pearson C.P., 2000, *MNRAS*, in press, astro-ph/0011335
- Peebles P.J.E., 1980, *The Large-Scale Structure of the Universe*, Princeton University Press
- Peebles P.J.E., 1993, *Principles of Physical Cosmology*, Princeton University Press
- Persic M., Salucci P., 1992, *MNRAS*, 258, 14
- Scott D., White M., 1999, *A&A*, 346, 1
- Sheth R.K., Tormen G., 1999, *MNRAS*, 308, 119
- Seljak U., Zaldarriaga M. 1996, *ApJ*, 469, 437.
- Smail I., Ivison R.J., Blain A.W., 1997, *ApJ*, 490, L5
- Smail I., Ivison R.J., Kneib J.-P., Cowie L.L., Blain A.W., Barger A.J., Owen F.N., Morrison G., 1999, *MNRAS*, 308, 1061
- Smail I., Ivison R.J., Owen F.N., Blain A.W., Kneib J.-P., 2000, proc. UMass/INAOE Conf. "Deep Millimeter Surveys", World Scientific, in press, astro-ph/0008237
- Somerville R.S., Lemson G., Sigad Y., Dekel A., Kauffmann G., White S.D.M., 2001, *MNRAS*, 320, 289
- Steidel C.C., Giavalisco M., Dickinson M., Adelberger K.L., 1996, *AJ*, 112, 352
- Takeuchi T.T., Ishii T.T., Hirashita H., Yoshikawa K., Matsuhara H., Kawara K., Okuda H., 2000, *PASJ*, in press, astro-ph/0009460
- Toffolatti L., Argueso Gomez F., De Zotti G., Mazzei P., Franceschini A., Danese L., Burigana C., 1998, *MNRAS*, 297, 117